**Supplementary Information**

# Apolipoprotein A-I structural organization in high density lipoproteins isolated from human plasma

Rong Huang[1], R. A. Gangani D. Silva[1], W. Gray Jerome[2], Anatol Kontush[3,4,5], M. John Chapman[3,4,5], Linda K. Curtiss[6], Timothy J. Hodges[7], and W. Sean Davidson[1]

[1]Department of Pathology and Laboratory Medicine, University of Cincinnati, Cincinnati, Ohio, USA. [2]Department of Pathology, Vanderbilt University Medical Center, Nashville, Tennessee, USA. [3]Université Pierre et Marie Curie - Paris 6, Paris, France. [4]National Institute of Health and Medical Research (INSERM) Dyslipoproteinemia and Atherosclerosis Research Unit (UMR 939), Paris, France. [5]Assistance Publique-Hopitaux de Paris, Groupe hospitalier Pitié - Salpétrière, Paris, France. [6]Department of Immunology and Vascular Biology, The Scripps Research Institute, La Jolla, California, USA. [7]Department of Mathematical Sciences, University of Cincinnati, Cincinnati, Ohio, USA.

**Corresponding author:**
W. Sean Davidson, Department of Pathology and Laboratory Medicine, University of Cincinnati, 2120 E. Galbraith Rd., Cincinnati, Ohio 45237-0507 USA Telephone: (513) 558-3707; Fax: (513) 558-1312; E-mail: Sean.Davidson@UC.edu

**Supplementary Figures**

1: Particle size characterization.

2: Correlation of particle diameters calculated from composition vs. experimental measurement.

3: Cross-linking of various LpA-I particles as a function of increasing concentrations of $BS^3$ cross-linker.

4: Correlation of particle diameters calculated from composition vs. experimental measurement.

5. Characterization of gel filtration isolated LpA-$I_{2b}$ and LpA-$I_{3b}$ and comparison of their cross-linking patterns.

6: Association constant of monoclonal antibody AI-115.1 to immobilized HDL subfractions by surface plasmon resonance.

7: Evaluation of the Double Super Helix (DSH) model in native LpA-I particles.

**Supplementary Tables**

1: Calculated number of molecules per particle for each of the major components of HDL.

2: Particle twist calculation parameters.

**Supplementary Methods**

**Supplementary References**

a

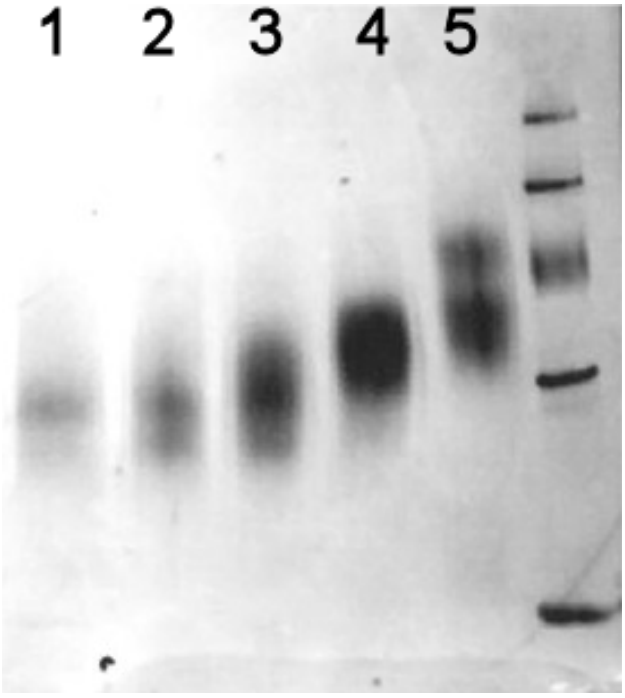


Nature Structural & Molecular Biology: doi:10.1038/nsmb.2028

b

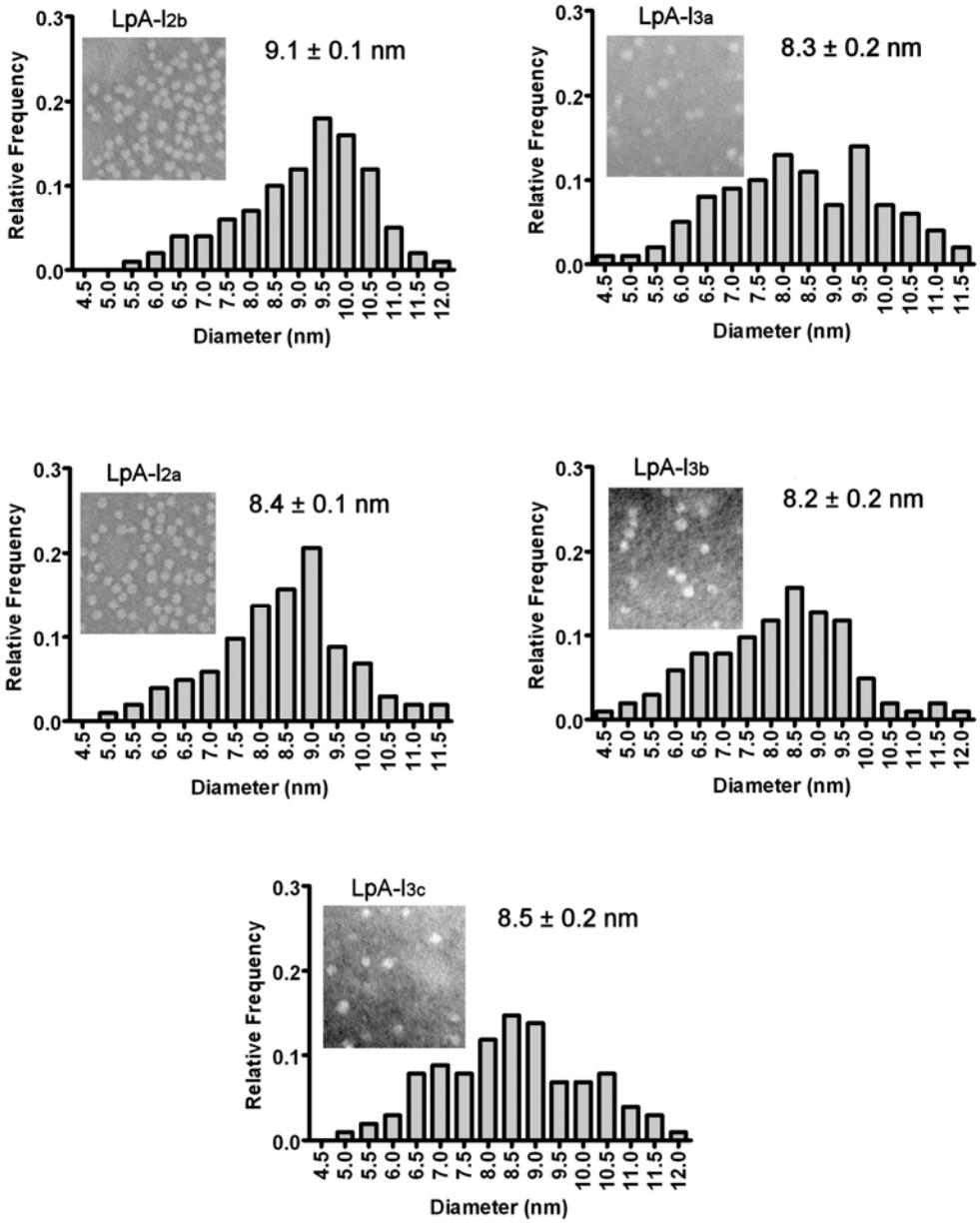


**Supplementary Figure 1: Particle size characterization.** (**a**) Representative native gel electrophoresis of five HDL subfractions (not LpA-I) obtained from a healthy normolipidemic control subject. Lane 1, $HDL_{3c}$; lane 2, $HDL_{3b}$; lane 3, $HDL_{3a}$; lane 4, $HDL_{2a}$; lane 5, $HDL_{2b}$ and standards (thyroglobulin, ferritin, catalase, LDH and albumin corresponding to 669, 440, 232, 140 and 66 kDa in the descending order). The calculated mean hydrated diameters of HDL subfractions are: 8.7 ± 0.3, 8.7 ± 0.2, 9.0 ± 0.3, 9.8 ± 0.5 and 11.3 ± 0.4 nm for HDL3c, 3b, 3a, 2a and 2b, respectively (mean ± standard deviation (S.D.) for 7 normolipidemic controls). (**b**) Negative stain electron microscopy of LpA-I samples from one healthy normolipidmic donor**.** Inset shows a negative stain image of the particles. Histograms were generated as described in **Supplementary Methods**. Average diameter as measured by image analysis is shown ± 1 S.D.

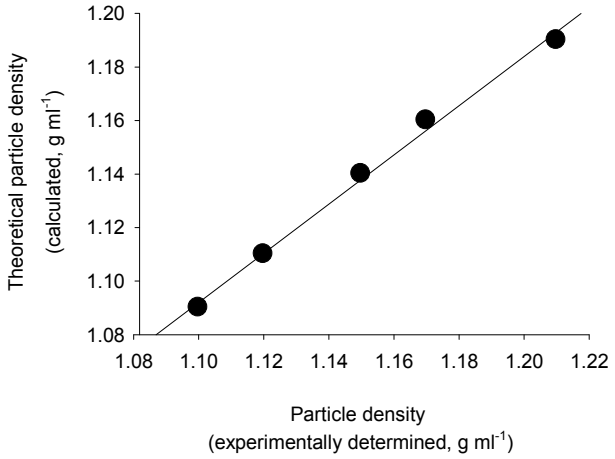


**Supplementary Figure 2: Correlation of particle densities calculated from composition vs. experimental measurement.** Correlation of experimentally determined particle density (*d*) in grams per ml (measured experimentally by dividing the volume of each HDL subfraction by its weight) with a predicted density derived from the following equation [1]:

$$d = \frac{100}{\frac{\%aa}{1.373} + \frac{\%PL}{1.031} + \frac{\%FC}{1.033} + \frac{\%TG}{0.915} + \frac{\%CE}{0.958}}$$

where %x represents the percent protein, phospholipid, free cholesterol, triglyceride or cholesteryl ester content by weight.

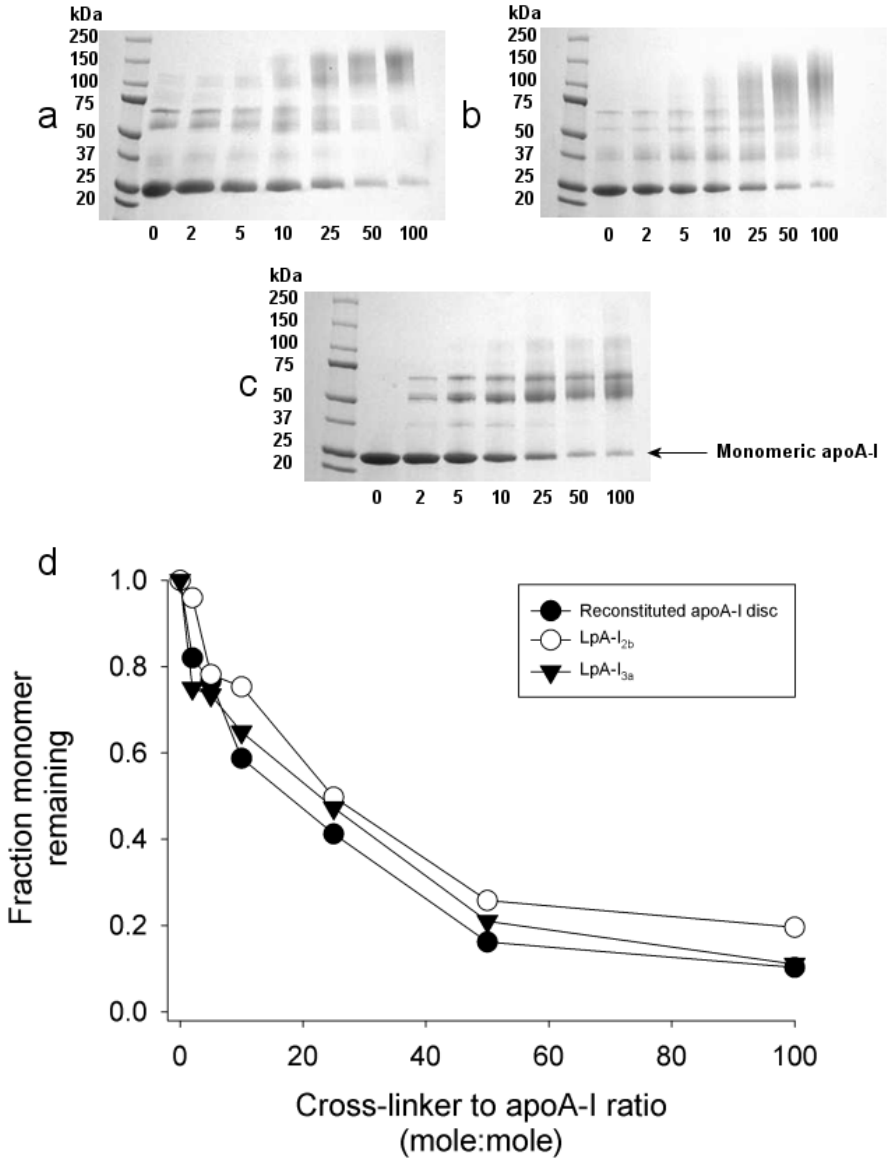


**Supplementary Figure 3: Cross-linking of LpA-I particles as a function of increasing concentrations of $BS^3$ cross-linker.** (**a**) 4-15% Tris-HCl SDS-PAGE gel of LpA-$I_{2b}$ incubated with increasing concentrations of $BS^3$ (molar ratio of $BS^3$ to apoA-I is shown below each lane). (**b**) LpA-$I_{3a}$ treated as in panel a. (**c**) A synthetic rHDL particle of 96 Å diameter with two molecules of apoA-I per particle and a composition of 80:8:1 (mole: mole phospholipid: unesterified cholesterol: apoA-I) treated as in panel a. All particles were cross-linked at 4 ºC for 16 h. The gels were stained with coomassie blue. *Note: The biological LpA-I samples all exhibited a small amount of dimer formation (Panels A and B, 0 lane) prior to the addition of the cross-linking reagent. We hypothesize that this represents background oxidative cross-linking possibly due to lipid peroxides present in the biological samples. (**d**) The monomeric apoA-I band in panels a-c was scanned by densitometry and the disappearance of each as a function of cross-linker concentration was plotted. The intensity of the monomeric band in the absence of cross-linker was set to 1.0 and each subsequent sample was scaled accordingly.

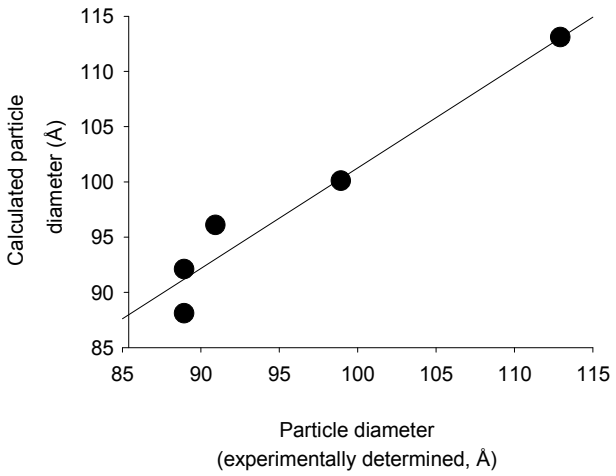


**Supplementary Figure 4: Correlation of particle diameters calculated from composition vs. experimental measurement.** Correlation of experimentally determined particle diameter (*D*, averaged value from the native PAGE and gel filtration estimation (**Table 1 in manuscript**)) with a predicted diameter determined from summation of the partial specific volumes for each component as reported in **Supplementary Table 1** using method of Duverger et al. [2].

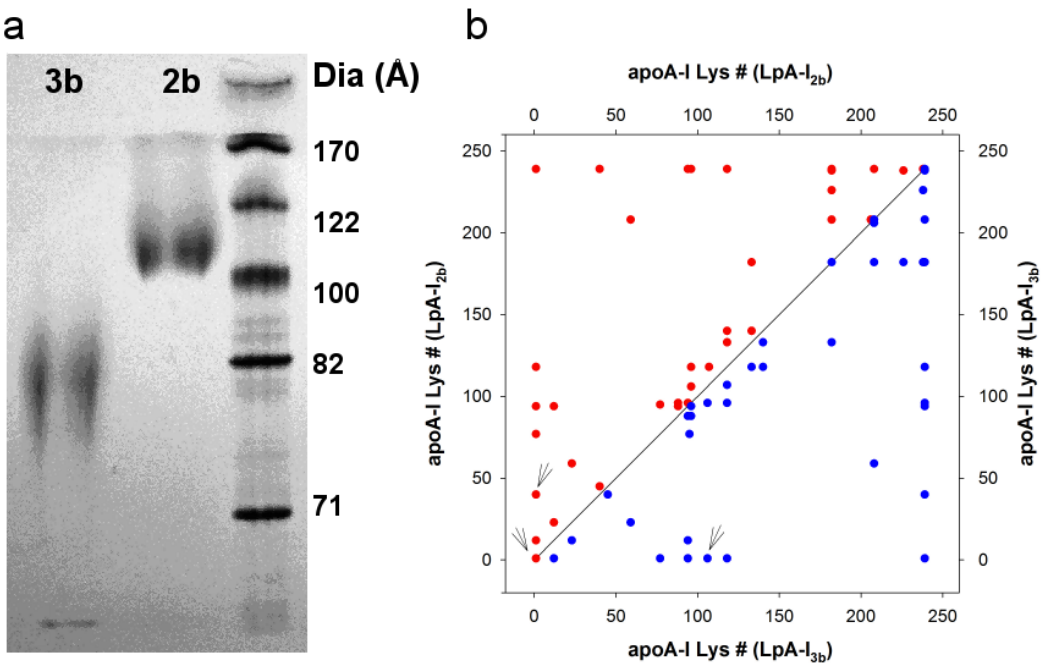


**Supplementary Figure 5: Characterization of gel filtration isolated LpA-$I_{2b}$ and LpA-$I_{3b}$ and comparison of their cross-linking patterns.** As described in the text, LpA-$I_{2b}$ and LpA-$I_{3b}$ fractions were isolated by ultracentrifugation and disulfide chromatography as described in Methods. Then, each was applied to a gel filtration setup containing three Superdex 200 columns (GE Healthcare) in series. The largest fractions corresponding to LpA-$I_{2b}$ and the smallest fractions corresponding to LpA-$I_{3b}$ were pooled, concentrated and analyzed. (**a**) An 8-25% native PAGE analysis of $BS^3$ cross-linked LpA-$I_{2b}$ and LpA-$I_{3b}$ showing no size overlap between the two preparations. (**b**) A plot of cross-linking patterns derived from the LpA-$I_{2b}$ (upper left, red) and LpA-$I_{3b}$ (lower right, blue). The X- and Y-axes show the Lys residue involved in a specific cross-link (both intra- and intermolecular, see **Table 2**). Cross-links indicated with an arrow were unique to either sample. These cross-links were verified with triplicate MS experiments. The high similarity of the cross-linking patterns on both sides of the unity line dividing the plot is clear. Overall, we found all 39 cross-links found in **Table 2**. In this particular experiment, 36 of these were found in both samples with one unique to LpA-$I_{3b}$ and two unique to LpA-$I_{2b}$.

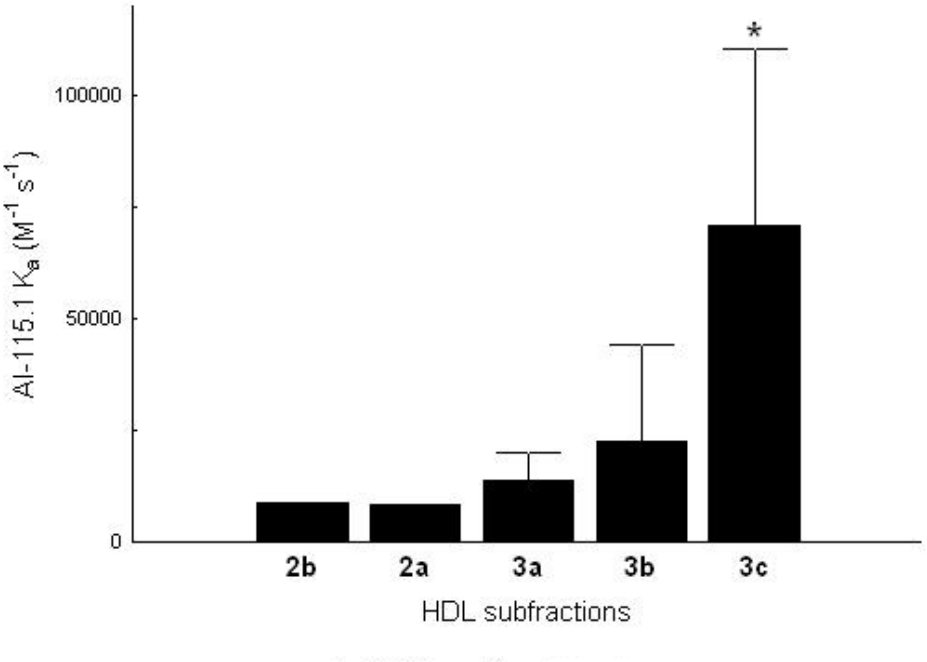


**Supplementary Figure 6: Association constant of monoclonal antibody AI-115.1 to immobilized HDL subfractions by surface plasmon resonance.** The monoclonal antibody AI-115.1 interacts with the central region of apoA-I between residues 115 and 126. Measurements are shown ± 1 S.D. (n=3) and statistically significant differences from the $HDL_{2b}$ data are noted with an asterisk at $p<0.05$ from an analysis of variance.

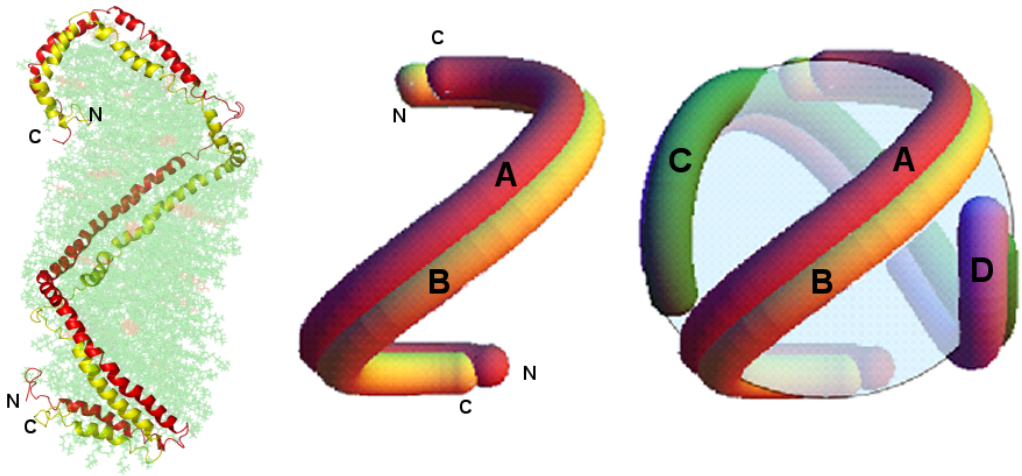


**Supplementary Figure 7: Evaluation of the Double Super Helix (DSH) model in native LpA-I particles**. Wu et al. recently proposed an apoA-I model in reconstituted particles where two antiparallel apoA-I molecules form an extended, cigar-shaped micellar arrangement instead of a bilayer disc [3], shown on the far left (provided by Stan Hazen, Cleveland Clinic). This model is consistent with the majority of our reported cross-linking results [4] and does not conflict with studies of helical orientation with respect to phospholipid acyl chains [5]. With respect to apoA-I, the major difference between the DSH and the double belt concept is that the N-termini and C-termini of each apoA-I molecule are far apart in the DSH, but close together in the double belt. The DSH can be modified to accommodate a spherical surface. If one refers to each end of an apoA-I DSH dimer (molecules A and B) as "top" and "bottom", one can imagine slightly unwinding and simultaneously compressing the top toward the bottom to distend the central region of the double helix so that it could wrap around a sphere (center and right schematics). In the case of an LpA-$I_{2a}$ particle, a second pair of antiparallel apoA-I molecules (molecules C and D) can be added in an orthogonal orientation. This puts four molecules of apoA-I in an arrangement that is consistent with the diameter of $HDL_{2a}$ and much, but not all, of our cross-linking data. Decreases in diameter could be affected as for the trefoil-based models by increasing the angle of twist. However, it is not clear to us how a version with odd numbers of molecules would work, unless the double helix is split to add unpaired molecules of apoA-I. Interestingly, if such a split were to be postulated, the result would be a model that looks very similar to the trefoil based models. Furthermore, it is difficult to rationalize our observed C-C and N-N cross-links in the context of this model (see text).

**Supplementary Table 1: Calculated number of molecules per particle for each of the major components of HDL.**

| Particle[a] | Phospho-lipid[b] | Cholesteryl ester[b] | Triglyceride[b] | Free cholesterol[b] | apoA-I molecules[c] |
|---|---|---|---|---|---|
| LpA-$I_{2b}$ | 170 | 143 | 23 | 53 | 5 |
| LpA-$I_{2a}$ | 103 | 87 | 15 | 25 | 4 |
| LpA-$I_{3a}$ | 78 | 64 | 13 | 17 | 4 |
| LpA-$I_{3b}$ | 59 | 49 | 10 | 12 | 4 |
| LpA-$I_{3c}$ | 39 | 31 | 9 | 9 | 4 |

[a] Components calculated as described in Methods.

[b] Calculated from values in **Table 1** which were obtained from two independent experiments and averaged.

[c] This number was derived by calculating a predicted particle diameter assuming a sphere using the weight percentage composition data for various putative numbers of apoA-I molecules per particle. The number of apoA-I molecules that resulted in a predicted particle diameter that best fit the experimental data is reported here. See **Fig. 2b** in the manuscript and related discussion.

**Supplementary Table 2: Particle twist calculations.** The total particle diameter, *A*; the radius *R* of the sphere on which the axes of the apoA-I helices lie; and the twist angle *Θ* required for the proteins to fit on the particle are shown (see Methods).

| Parameter | LpA-$I_{2b}$ | LpA-$I_{2a}$ | LpA-$I_{3a}$ | LpA-$I_{3b}$ | LpA-$I_{3c}$ |
|---|---|---|---|---|---|
| *A* (Å) | 112 | 98 | 90 | 88 | 88 |
| *R* (Å) | 50.5 | 43.5 | 39.5 | 38.5 | 38.5 |
| *Θ* (radians) | 0 | 0.82 | 1.21 | 1.31 | 1.31 |

## Supplementary Methods

**Sulfhydryl covalent chromatography** HDL subfractions obtained from density ultracentrifugation were dialyzed into 10 mM DTT-containing STB (pH was adjusted from 8.5 to 7.5 for maximum DTT reduction efficiency) for 2 h followed by another 2 h dialysis in 2 mM DTT-containing STB (pH 7.5) at 4 °C. Taking consideration of the amount of apoA-II in the sample and the DTT present, we then used a 15-fold excess of swollen thiopropyl sepharose resin (TPS; GE Healthcare). An appropriate amount of STB was used to resuspend the resin and half of the mixture was taken into a beaker and mixed with the DTT-reduced HDL subfractions for 20 min and then the reacted-resin was layered with the un-reacted resin in a 20 mL plastic column (BD, Franklin Lakes, NJ). After a 5 min settling time, the column was washed with STB and the flow-through fractions (LpA-I) were pooled and concentrated for subsequent cross-linking experiments. SDS PAGE was used to evaluate the separation efficiency of LpA-I from LpA-I/A-II HDL particles by the relative abundance of the apoA-II band.

**Negative stain electron microscopy** LpA-I subfractions were negatively stained for electron microscopy by floating formvar-carbon-coated copper electron microscopy grids for 20 seconds on a 40 microliter droplet of particles in buffer. Excess fluid was removed from the grids. The grids, with adsorbed particles, were floated on a 40 microliter droplet of 1% phosphotungstic acid stain at pH 6.1 for 20 seconds. Excess stain was removed and the dried grids were viewed at 80 KeV with an FEI CM-12 transmission electron microscope. To determine the particle diameters, images were collected randomly from the sample. From each image, 5-10 particles were randomly selected for measurement. This process was continued until 200 particles had been measured for each condition. For spherical particles, the diameter was taken as the longest visible axis. Particles having diameters of more than 2 standard deviations from the largest or smallest contiguous size classes were excluded from the analysis as outliers. Such particles were rare and totaled less than 1% of particles measured. The microscope magnification was calibrated immediately before images were obtained.

**Circular dichroism (CD)** LpA-I particle solutions were dialyzed against 20 mM phosphate buffer (PB) at pH 8.0 and the protein concentration was determined using the Markwell modified Lowry method [6]. To perform CD measurements, sample solutions were diluted to 150 μg $ml^{-1}$ with 20 mM PB, which were verified by $A_{280}$ measurements. CD spectra of LpA-I subfractions were measured on a J-715 spectrometer (Jasco, Easton, MD) using a 1 mm quartz CD cell (Starna, Inc.). The spectra were collected between 250-185 nm and measured as an average of three scans with a scan rate of 50 nm/min and a bandwidth of 1.0 nm with a time response of 2 s. Buffer spectra collected under the same conditions were subtracted to obtain the final spectra. The helicity of apoA-I in all LpA-I particles was estimated using the SELCON 3 method (a component of the CDPro software package at http://lamar.colostate.edu/~sreeram/CDPro/main.html).

**Limited proteolysis** Sequencing grade modified trypsin (Cat. # V5111, Promega, Madison, WI) was added to 1 mg $ml^{-1}$ LpA-I subfractions at a 100:1 protein:enzyme mass ratio and the limited proteolysis was performed at 37 °C in a water bath. At various time points (up to 1 h), aliquots of the sample solution was taken out from the reaction mixture and quenched by adding SDS and boiled for 3 min. The resulting samples were stored at -20 °C for later SDS PAGE analysis.

**Surface plasmon resonance and monoclonal AB binding** AI-115.1, a previously characterized epitope-defined monoclonal antibody to apoA-I, was used to probe the conformation of apoA-I in HDL subpopulations [7]. The association rate constants of the antibody were measured using surface plasmon resonance analysis as described elsewhere [7]. All measurements were obtained on a BIAcore 2000 system (Pharmacia Biosensor AB, Uppsala, Sweden).

**Cross-linking and processing samples for mass spectrometry** Particles were cross-linked at 1 mg $mg^{-1}$ apoA-I in PBS with $BS^3$ at a molar ratio of protein to cross-linker of 1:50. The reaction was carried out at 4 °C for 16 h when it was quenched by adding 1 M Tris·HCl (pH 8) to a final concentration of 100 mM. After

dialyzing into 10 mM ammonium bicarbonate (pH 8.1) and lyophilizing, the samples were subjected to a chloroform/methanol delipidation procedure. The resultant protein samples were resuspended in 200 µl STB with 3 M guanidine hydrochloride and then dialyzed extensively into 10 mM ammonium bicarbonate (pH 8.1). The samples were digested by 2.5% (w/w) trypsin/apoA-I at 37 °C overnight. A second 2.5% (w/w) trypsin was added the next morning for an additional 2 h. After digestion, aliquots of the samples (50 µg) were lyophilized and stored at -20 °C for mass spectrometric measurement.

**Mass spectrometric measurements and data analysis** Tryptic peptides were first separated with an on-line capillary HPLC (Agilent 1100) prior to detection on a QStar XL mass spectrometer equipped with an electrospray ionizer and a quadropole time-of-flight dual analyzer. Briefly, the samples were suspended in 0.1% (v/v) trifluoroacetic acid (TFA) at a protein concentration of 2 µg $\mu l^{-1}$. 30 pmol of sample (assuming apoA-I) was injected onto a C18 (Vydac 0.5 mm id x 15 cm) column for separation with a gradient of 0-40% (v/v) acetonitrile in water over 120 min at a flow rate of 6 µl $min^{-1}$. The eluted peaks were subjected to mass spectrometric detection within a range of 300-1800 m/z. In addition, MS/MS sequencing was performed in the range of 100-2000 m/z in Q2 pulsing mode using the Information Dependent Acquisition (IDA) feature in the Analyst QS software. The MS instrument was calibrated externally using purified apoA-I tryptic digested peptides.

We generated a list of experimental masses for peptides that had been subjected to MS/MS fragmentation using the Mascot script in the AnalystQS 1.1 software (Applied Biosystems). This list was compared to a theoretical list of apoA-I tryptic peptides that were either unmodified, containing one or more hydrolyzed cross-linkers, or one or more intra- or inter-molecular cross-links using our in house program, Cross ID. All putative cross-links predicted by mass were then verified by manual evaluation of the corresponding MS/MS spectrum.

**Particle volume, diameter and surface area calculations** Knowing the molar ratio of each lipid component with respect to apoA-I (calculated from **Table 1**), we summed the partial specific volumes for each chemical component to calculate a hypothetical diameter for each particle. We used the following molecular volumes for this calculation: amino acid, 2.32 $Å^3$ per Dalton [8]; phospholipid, 1270 $Å^3$, cholesterol, 600 $Å^3$, cholesteryl ester, 1090 $Å^3$, and triglyceride, 1600 $Å^3$ [9]. This summed volume was calculated for various putative numbers of apoA-I molecules per particle. We then calculated a theoretical particle diameter (*D*) from the following equation:

$$D = 2r = 2 \times \sqrt[3]{\frac{3V}{4\pi}} \qquad (1)$$

where *V* is the summed volumes of all chemical components assuming a given number of apoA-I molecules per particle. This diameter was then compared to the experimentally measured diameter averaged from native PAGE and gel filtration in **Table 1** for each LpA-I particle. The number of apoA-I molecules that provided the hypothetical diameter that most closely matched the experimental value and fell within the range of potential apoA-I molecules per particle as determined by chemical cross-linking (**Fig. 2**) was selected as the correct value. Given this analysis **Supplementary Table 1** reflects the average number of each major chemical component for the LpA-I species. For particle surface area calculations, we used values of 40 $Å^2$ for free cholesterol and 65 $Å^2$ for phospholipid. These values were determined from surface chemistry experiments at surface packing pressures of 25 dyn $cm^{-1}$ of $HDL_3$ lipids [10]. Using the compositional data in **Supplementary Table 1**, the total surface areas of cholesterol and phospholipid were summed and expressed as a percentage of the total surface area of a sphere with the experimentally determined diameter reported for each LpA-I particle in **Table 1**.

**Supplementary References**


1. Castle,C.K. *et al.* Remodeling of the HDL in NIDDM: a fundamental role for cholesteryl ester transfer protein. *Am. J. Physiol* **274**, E1091-E1098 (1998).

2. Duverger,N. *et al.* Biochemical characterization of the three major subclasses of lipoprotein A-I preparatively isolated from human plasma. *Biochemistry* **32**, 12372-12379 (1993).

3. Wu,Z. *et al.* Double superhelix model of high density lipoprotein. *J. Biol. Chem.* **284**, 36605-36619 (2009).

4. Silva,R.A., Hilliard,G.M., Li,L., Segrest,J.P., & Davidson,W.S. A mass spectrometric determination of the conformation of dimeric apolipoprotein A-I in discoidal high density lipoproteins. *Biochemistry* **44**, 8600-8607 (2005).

5. Panagotopulos,S.E., Horace,E.M., Maiorano,J.N., & Davidson,W.S. Apoliprotein A-I adopts a belt-like orientation in reconstituted high density lipoproteins. *J. Biol. Chem.* **276**, 42965-42970 (2001).

6. Markwell,M.A., Haas,S.M., Bieber,L.L., & Tolbert,N.E. A modification of the Lowry procedure to simplify protein determination in membrane and lipoprotein samples. *Anal. Biochem.* **87**, 206-210 (1978).

7. Curtiss,L.K., Bonnet,D.J., & Rye,K.A. The conformation of apolipoprotein A-I in high-density lipoproteins is influenced by core lipid composition and particle size: a surface plasmon resonance study. *Biochemistry* **39**, 5712-5721 (2000).

8. Matthews,B.W. Solvent content of protein crystals. *J. Mol. Biol.* **33**, 491-497 (1968).

9. Edelstein,C., Kezdy,F.J., Scanu,A.M., & Shen,B.W. Apolipoproteins and the structural organization of plasma lipoproteins: human plasma high density lipoprotein-3. *J. Lipid Res.* **20**, 143-153 (1979).

10. Ibdah,J.A., Lund-Katz,S., & Phillips,M.C. Molecular packing of high-density and low-density lipoprotein surface lipids and apolipoprotein A-I binding. *Biochemistry* **28**, 1126-1133 (1989).